

A sensor fault detection strategy for structural health monitoring systems

Chia-Ming Chang^{*1}, Jau-Yu Chou^{1a}, Ping Tan^{2b} and Lei Wang^{2c}

¹Department of Civil Engineering, National Taiwan University, Taipei 10617, Taiwan

²Earthquake Engineering Research & Test Center, Guangzhou University, Guangzhou 510405, China

(Received November 15, 2016, Revised April 26, 2017, Accepted May 9, 2017)

Abstract. Structural health monitoring has drawn great attention in the field of civil engineering in past two decades. These structural health monitoring methods evaluate structural integrity through high-quality sensor measurements of structures. Due to electronic deterioration or aging problems, sensors may yield biased signals. Therefore, the objective of this study is to develop a fault detection method that identifies malfunctioning sensors in a sensor network. This method exploits the autoregressive modeling technique to generate a bank of Kalman estimators, and the faulty sensors are then recognized by comparing the measurements with these estimated signals. Three types of faults are considered in this study including the additive, multiplicative, and slowly drifting faults. To assess the effectiveness of detecting faulty sensors, a numerical example is provided, while an experimental investigation with faults added artificially is studied. As a result, the proposed method is capable of determining the faulty occurrences and types.

Keywords: sensor fault detection; autoregressive modeling; a bank of Kalman estimators

1. Introduction

The process of assessing structural deteriorates is referred to as structural health monitoring (SHM). In past two decades, SHM has gained considerable attention due to the need of understanding and maintaining infrastructure systems (Brownjohn 2006). Numerous SHM methods have been developed and experimentally verified on laboratory- and full-scale structures, as well as various long-term monitoring systems have been deployed in structures (Farrar and James 1997, Beck *et al.* 1998, Peeters and De Roeck 2001, Park *et al.* 2005, Feng 2009, Xu *et al.* 2015, Xia and Ni 2016). In these SHM applications, sensors are assumed to be always well functioning. To our best knowledge, only a minority of studies have mentioned the significance of the sensor fault diagnosis in a SHM sensor network.

In most SHM applications, the characterization of structures relies on the high-quality sensor measurements. A defective sensor would result in a false condition of structures and lead engineers to make incorrect decisions. Wang *et al.* (2015) mentioned that sensor errors and faulty signals may potentially lead structures in vibration to catastrophic failures. As indicated in Rice and Spencer (2009), the performance of sensors is evaluated by their

sensitivity, linearity, and drift. Due to the lifetime, a degrading sensor would lower its sensing capability on these performance factors. Moreover, sensors may also be subjected to man-made damage, natural wearing, aging, and careless maintenance, resulting in a failure of sensing capability. In SHM applications, sensors instrumented on a structure should be regularly checked to assure their functionality.

Alternatively, a stochastic model, which estimates structural responses, can be used to locate faulty sensors instrumented on a structure. In time series analysis, the autoregressive (AR) model is one type of stochastic modeling techniques that estimates the current or one-step ahead responses of structures by a linear combination of delayed outputs (Liao *et al.* 2016, Nardi *et al.* 2016, Busca *et al.* 2015, Lynch *et al.* 2004). In the literature, Sohn *et al.* (2000) applied this modeling technique to an undamaged structure and used the derived coefficients to detect damage in the structure. Yah and Pakzad (2012) calculated the residuals between the AR model and the measured data with a combination of the Ljung-Box statistic technique as damage index. Park *et al.* (2016) focused on the system identification of reinforced concrete bridges using the vector autoregressive model technique. As a sensor in a sensor network becomes defective, the residuals between the estimated responses and measured signals will be significantly changed and then turn into a non-Gaussian process. These sudden changes can be employed as an indicator of faulty sensors based on the AR modeling technique.

The Kalman filtering technique has a wide variety of applications in the SHM field. Lei *et al.* (2015) developed a two-stage damage detection method by integrating the Kalman estimator approach and least-squares estimation. Lei *et al.* (2016) improved the Kalman filter to identify the

*Corresponding author, Assistant Professor

E-mail: changcm@ntu.edu.tw

^a Graduate student

E-mail: r04521251@ntu.edu.tw

^b Professor

E-mail: ptan@gzhu.edu.cn

^c Ph.D.

E-mail: 119827293@qq.com

unknown input and responses of structures. In this method, different types of measurements were employed to enhance the identification quality. Kim *et al.* (2016) implemented a two-stage Kalman estimator to compute dynamic displacements from acceleration measurements. Palanisamy *et al.* (2015) experimentally validated the strain estimation using the Kalman filtering technique when the structure is excited by a nonzero mean input. A Kalman estimator can be constructed from the system identification result (e.g., the result from the AR modeling technique) and can be further used in other applications.

Moreover, another type of Kalman filtering applications is to derive a bank of Kalman estimators for fault detection (Pbrianti *et al.* 2016, Lim and Park 2014, Saravanakumar *et al.* 2014). A bank of Kalman filters were proposed to address the aircraft engine sensor failures by the NASA's Advanced Detection, Isolation, and Accommodation Program in the 1980's (Merrill *et al.* 1988). This program successfully exhibited the use of a bank of Kalman filters for improving the control loop tolerance to sensor failures. Later, many studies were carried to further improve this method for the fault detection and isolation problems, in particular of aircraft engine sensing systems (Hanlon and Maybeck 2000, Kobayashi and Simon 2005). In addition, each Kalman filter in a bank is able to predict structural responses using full or partial sensor measurements so as the response at a specific sensor location can be estimated from different sets of sensor measurements. By comparing among the responses, a bank of Kalman filters recognize faulty sensors and fault types in a sensor network.

The objective of this study is to develop a sensor fault detection method based on the output measurements of a structure. This method first exploits the autoregressive modeling technique to identify a stochastic representation of a structure in accordance with the sensor measurements. Subsequently, multiple Kalman estimators (or filters) are established based on this stochastic model. Because the conversion may result in unstable poles, all the estimators are refined by the deterministic discrete-time Kalman estimation method. This study assumes that the additive, multiplicative, and slowly drifting faults would occur in defective sensors (Qin and Li 1999, Abdelghani and Friswell 2007, Heredia *et al.* 2008, 2011). The additive fault occurs when an unexpected bias is added to the sensor signal. Changed power to sensors can result in the multiplicative fault. The slowly drifting fault can be found in aging sensors. Note that sensor faults are not limited to these three types. A numerical simulation is conducted to assess performance of the proposed method, while the data collected from an experiment are used to validate the method by adding faulty signal artificially. Consequently, the proposed method is capable of diagnose the fault type and occurrence time of the defective sensors.

2. Sensor fault detection

Sensor fault detection can be accomplished by comparing estimated responses with measured responses of a structure. In this study, the estimated responses are

derived from a bank of Kalman estimators of which each is converted from the AR modelling technique. Note that these Kalman estimators are established when all sensors are in a normally functioning condition. The faulty sensors are then identified by the variations of the residuals between the estimated and measured responses. The fault types and time of occurrence are eventually determined based on the residuals.

Fig. 1 displays the flowchart of the proposed sensor fault detection method. This flowchart consists of an AR model, an AR-Kalman convertor, a bank of Kalman estimators, and fault recognition. Each component is introduced in details in the following sections.

2.1 Autoregressive modeling (AR)

The autoregressive modeling technique is employed to develop a stochastic model of a structure that estimates responses at the sensor locations. The stochastic model estimates the responses using the delayed measurements. The number of delays can be predetermined empirically or by some criteria, e.g., Akaike's information criterion (Akaike 1974) or Bayesian information criterion (Akaike 1977). Once the number of delays is appropriately determined, a stochastic representation of an instrumented structure can be obtained by the AR modeling technique.

The autoregressive modelling is briefly reviewed. Assume that m -channel measurements of a structures have n samples. Thus, these data are used to derive an AR model that estimates the current responses by the previous measurements. The AR model is then written by

$$\mathbf{y}[k] = \sum_{i=1}^p \mathbf{A}_i \mathbf{y}[k-i] + \mathbf{e}[k] \quad (1)$$

Where $\mathbf{y}[k] \in^{m \times 1}$ is a vector of the sensor measurements at the time step k ; \mathbf{A}_i are the matrix coefficients with respect to $\mathbf{y}[k-i]$; p is the number of delays; $\mathbf{e}[k]$ is a vector of the measurement noise that can be also interpreted as the modeling errors. For a multiple output system, the matrix coefficients can be obtained by

$$\mathbf{Y} = [\mathbf{A}_1, \mathbf{A}_2, \dots, \mathbf{A}_p] \mathbf{X} \quad (2)$$

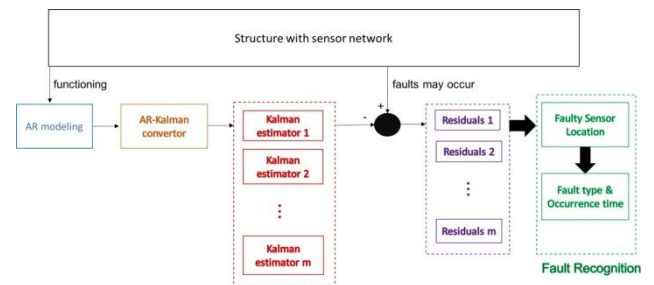


Fig. 1 Flowchart of the proposed sensor fault detection method

where

$$\mathbf{Y} = [\mathbf{y}[p+1], \mathbf{y}[p+2], \dots, \mathbf{y}[n]] \quad (3)$$

$$\mathbf{X} = \begin{bmatrix} \mathbf{y}[p] & \mathbf{y}[p+1] & \dots & \mathbf{y}[n-1] \\ \mathbf{y}[p-1] & \mathbf{y}[p] & \dots & \mathbf{y}[n-2] \\ \vdots & \vdots & \ddots & \vdots \\ \mathbf{y}[1] & \mathbf{y}[2] & \dots & \mathbf{y}[n-p] \end{bmatrix} \quad (4)$$

All matrix coefficients in this multiple output system are solved by the matrix pseudoinverse such as

$$[\mathbf{A}_1, \mathbf{A}_2, \dots, \mathbf{A}_p] = \mathbf{Y}\mathbf{X}^\dagger \quad (5)$$

where † indicates the pseudo inverse operator. With these matrix coefficients, the AR model is ready to estimate the responses by the delayed measurements such as Eq. (1).

2.2 Kalman estimator

A Kalman estimator serves as an optimal observation of a system in which the one-step ahead response can be evolutionarily estimated by the current measurements. As compared to the AR model, Kalman estimators can exploit different numbers of responses as the inputs and outputs. With a specific input-output relationship, a bank of Kalman estimators are established to detect faulty sensors in a sensor network.

The derivation of Kalman estimators are briefly introduced. First, a stochastic state-space model can be represented as

$$\begin{aligned} \mathbf{x}[k+1] &= \mathbf{A}\mathbf{x}[k] + \boldsymbol{\omega}[k] \\ \mathbf{y}[k] &= \mathbf{C}\mathbf{x}[k] + \mathbf{v}[k] \end{aligned} \quad (6)$$

where \mathbf{A} is the system matrix; \mathbf{C} is the output matrix; \mathbf{x} is the state vector; \mathbf{y} is the output vector; $\boldsymbol{\omega}$ and \mathbf{v} are the disturbance and measurement noise. In Eq. (6), the output vector can represent the measurements at sensor locations. Because Kalman estimators are an alternative type of stochastic representation of a structure, these estimators are then derived from the AR model and given by

$$\begin{aligned} \hat{\mathbf{x}}[k+1] &= \mathbf{A}_d \hat{\mathbf{x}}[k] + \mathbf{K}\mathbf{e}[k] \\ \hat{\mathbf{y}}[k] &= \mathbf{C}\hat{\mathbf{x}}[k] \\ \mathbf{e}[k] &= \mathbf{y}[k] - \hat{\mathbf{y}}[k] \end{aligned} \quad (7)$$

where

$$\begin{aligned} \mathbf{x}[k] &= [\mathbf{y}^T[k-p+1] \quad \mathbf{y}^T[k-p+2] \quad \dots \quad \mathbf{y}^T[k]]^T \\ \mathbf{A}_d &= \begin{bmatrix} \mathbf{0} & \mathbf{I} & \mathbf{0} & \mathbf{0} \\ \mathbf{0} & \mathbf{0} & \mathbf{I} & \mathbf{0} \\ \vdots & \vdots & \ddots & \vdots \\ \mathbf{A}_p & \mathbf{A}_{p-1} & \dots & \mathbf{A}_1 \end{bmatrix}, \mathbf{K} = \begin{bmatrix} \mathbf{0} \\ \mathbf{0} \\ \vdots \\ \mathbf{I} \end{bmatrix}, \mathbf{C} = [\mathbf{0} \quad \mathbf{0} \quad \dots \quad \mathbf{I}] \end{aligned} \quad (8)$$

Eqs. (7) and (8) are the state-space representation of a Kalman estimator converted from an AR model. By merging the estimation errors to the system equation, Eq. (7) can be rewritten by

$$\begin{aligned} \hat{\mathbf{x}}[k+1] &= (\mathbf{A}_d - \mathbf{K}\mathbf{C})\hat{\mathbf{x}}[k] + \mathbf{K}\mathbf{y}[k] \\ \hat{\mathbf{y}}[k+1] &= \mathbf{C}\hat{\mathbf{x}}[k+1] \end{aligned} \quad (9)$$

where $\hat{\mathbf{y}}[k+1]$ indicates the one-step ahead estimation. Unfortunately, the derived Kalman estimator in Eq. (9) is only adequate for an m -input and m -output estimation.

For different numbers of inputs and outputs, the Kalman gain, \mathbf{K} , should be modified. The deterministic Kalman estimator can be used to derive a new Kalman gain using Eq. (7). For example, the system matrix used in the deterministic Kalman estimator is still \mathbf{A}_d , while the measurement matrix can be a part of \mathbf{C} (e.g., some rows in \mathbf{C}) and defined as $\bar{\mathbf{C}}$. The disturbance and measurement noise covariance matrices, \mathbf{Q} and \mathbf{R} , are identical to the covariance of $\mathbf{e}[k]$ in Eq. (1). Thus, the refined Kalman estimator is written by

$$\begin{aligned} \hat{\hat{\mathbf{x}}}[k+1] &= (\mathbf{A}_d - \mathbf{L}\bar{\mathbf{C}})\hat{\hat{\mathbf{x}}}[k] + \mathbf{L}\bar{\mathbf{y}}[k] \\ \hat{\hat{\mathbf{y}}}[k+1] &= \bar{\mathbf{C}}\hat{\hat{\mathbf{x}}}[k+1] \\ \hat{\mathbf{y}}[k+1] &= \mathbf{C}\hat{\hat{\mathbf{x}}}[k+1] \\ \mathbf{R}[k] &= \hat{\mathbf{y}}[k] - \mathbf{y}[k] \end{aligned} \quad (10)$$

where $\bar{\mathbf{y}}[k]$ is a part of $\mathbf{y}[k]$, and $\mathbf{R}[k]$ is the residual between the measured and estimated responses. Finally, the estimated output can be the partial measurements, $\hat{\hat{\mathbf{y}}}$, or the full measurements, $\hat{\mathbf{y}}$. A bank of Kalman estimators are consequently established with various combinations.

2.3 Fault detection

Due to the lifetime and unexpected damage, sensors may return incorrect signals in measurements. In this study, three types of sensor faults are considered: the additive, multiplicative, and slowly drifting faults. Note that this study doesn't take the short-time pulse-like fault in account. These faults can also be represented in a mathematical form and listed in the following.

1. **Additive fault:** a constant offset is added to the correct sensor measurement(s) such as

$$y_j^f[l] = y_j[l] + \Delta_j, \quad l \geq t_f \quad (11)$$

Where y_j^f is the signal with an additive fault at the j -th sensor; l is an arbitrary time step; Δ_j is the constant offset at the j -th sensor; t_f is the time of the fault occurrence.

2. **Multiplicative fault:** the correct sensor measurement is amplified by a constant multiplier such as

$$y_j^f[l] = \alpha_j y_j[l], \quad l \geq t_f \quad (12)$$

where y_j^f is the signal with a multiplicative fault at the j -th sensor; l is an arbitrary time step; α_j is the constant gain at the j -th sensor; t_f is the time of the fault occurrence.

3. Slowly drifting fault: the correct sensor measurement is drifted at a rate of change such as

$$y_j^f[l] = y_j[l] + \beta_j(l - t_f), \quad l \geq t_f \quad (13)$$

where y_j^f is the signal with a slowly drifting fault at the j -th sensor; l is an arbitrary time step; β_j is the rate of change at the j -th sensor; t_f is the time of the fault occurrence. All types of faults are illustrated in Fig. 2.

As illustrated in Fig. 1, the proposed fault detection method utilizes a bank of Kalman estimators to identify malfunctioning sensors. The AR model in Eq. (1) is first developed using the measurements in a sensor network when all sensors work normally. This model is then converted to a Kalman estimator in Eq. (7) which acquires full measurements and estimates one-step ahead measurements of all sensors. To generate an estimator, the deterministic Kalman estimator in Eq. (10) is used with different numbers of inputs and outputs. By differentiating the number of inputs and outputs, a bank of Kalman estimators are established to detect faulty sensors.

For a structure, a specific bank of Kalman estimators are designed to inspect the condition of sensors in a sensor network. Assume that the total number of sensors is m . In the bank of Kalman estimators, each has $m-1$ inputs and m outputs of which the missing input is the sensor measurement to be identified as a defective sensor. When all sensors are in good condition, this bank of Kalman estimators can well estimate the one-step ahead outputs. However, if the j -th sensor becomes defective, the estimator without this j -th sensor in the input still yields a good estimation of all measurements. The other estimators will have incorrectly estimated responses due to the defective j -th sensor. The comparison on the measured and estimated responses identifies the faulty sensor in a sensor network, and the proposed method observes the residuals, i.e., $\hat{\mathbf{y}} - \mathbf{y}$ in Eq. (10), to detect this faulty sensor.

When the additive fault occurs in a sensor, the Kalman estimator, which is capable of detecting this faulty sensor, will render a pulse and then generate a constant offset in the residual time history. This pulse is because the Kalman estimator is unable to correctly estimate the response, while the constant offset is consistent with Δ_j in Eq. (11) after t_f . The pulse and constant offset are used to diagnose the time of fault occurrence and type in the proposed method.

When the multiplicative fault is introduced in a sensor, the Kalman estimator, which is capable of detecting this faulty sensor, will induce a pulse in the beginning and then oscillate in the residual time history. These two types of phenomena determine the time of fault occurrence and type.

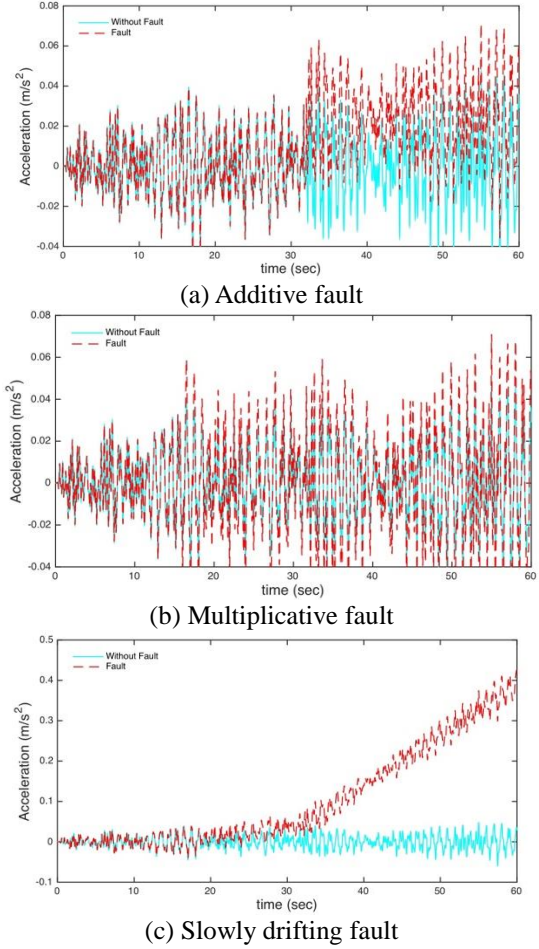


Fig. 2 Illustration of sensor faults

When the slowly drifting fault is found in a sensor, the Kalman estimator will produce a drifting residual. For this fault type, the time of occurrence is hard to be determined because the drifting residual will be unobvious in the beginning. After a certain length of time, the constantly drifting residual indicates the fault type of the defective sensor. The correct time of fault occurrence can be then determined.

The AR modeling method should have a sufficient length of measurements to identify the matrix coefficients in Eq. (1). The length of measurements must be greater than or equal to $p+m-1$ for an AR model which has m sensors and p delays. Nevertheless, the length of measurements is recommended to be 2~3 times of $p+m-1$ longer because the resolution can be improved and $e[k]$ in Eq. (1) would be close to the sensor noise. An accurate AR model helps the derived Kalman estimators capable of detecting the faulty sensors.

The deterministic Kalman estimator method used in this research not only changes the numbers of inputs and outputs in an estimator but also stabilizes the poles outside a unit circle in \mathbf{A}_d in Eq. (7). The AR modeling method does not guarantee all poles to be stable. The deterministic Kalman estimator method stabilizes these unstable poles by $\mathbf{A}_d - \mathbf{L}\bar{\mathbf{C}}$ in Eq. (10). Therefore, each estimator produces

convergent responses.

In this research, the faulty sensors are assumed to sequentially occur. In a sensor network, the faulty sensors, which concurrently occurs, is highly unlikely. Because the proposed method is able to identify the occurrence and type of a faulty sensor, signals measured from this faulty sensor can be temporarily corrected before this sensor has been fixed or replaced. If another sensor is found with a fault, the bank of Kalman estimators can still function to diagnose this defective sensor in a sensor network.

One concern about the proposed sensor fault detection method is to mistake measurements of a damaged structure as sensor faults. Measurements of a structure with slight damage may still contain similar dynamic characteristics, while readings from a faulty sensor would have irrelevant signals from the dynamics of structures. Thus, the proposed method can still work for slightly damaged structure. If the structure has sufficient severity of damage, the fault detection may be distorted. The proposed method is limited to be implemented when the structure is under healthy conditions or slightly damaged.

To sum up, the procedure of the proposed sensor fault detection method is listed in the following.

1. Construct an AR model using Eqs. (1)-(5) and the measured data when all sensors work normally.
2. Convert this AR model into a Kalman estimator with inputs and outputs identical to all sensors in Eqs. (7) and (8).
3. Generate a bank of Kalman estimators using Eq. (10). In these Kalman estimators, the number of inputs and outputs are defined as $m-1$ and m where m is the total number of sensors.
4. Implement the bank of Kalman estimators and calculate the residual between the estimated and measured responses. The location, time of occurrence, and fault type of faulty sensors are determined by the aforementioned approaches.

3. Numerical example

A five-story lumped-mass building is selected as the numerical example to examine the proposed sensor fault detection method. Fig. 3 illustrates the building with accelerometers installed on each floor. In the simulation, only the lateral responses are considered. For this building, the natural frequencies are 1.01 Hz, 2.93 Hz, 4.63 Hz, 5.94 Hz, 6.78 Hz, while the damping is assumed to be 2%. The excitation to this building is band-limited white noise with a variance of 1 m/sec^2 , and the sampling rate is set to be 200 Hz. The measured accelerations are added with white noise of which the variance is $2.2 \times 10^{-3} \text{ m/sec}^2$, resulting in 20 dB roughly in the signal-to-noise ratio. The simulation duration is 60 seconds. The simulation results without any faulty signals are demonstrated in Fig. 4.

The proposed sensor fault detection is implemented using the procedure in Section 2.3. In the 60-second measurements, the data in the first 15 seconds are used to develop the AR model in Eq. (1). This AR model is subsequently converted into a Kalman estimator by Eq. (7).

The number of delays used in this AR model is 7. A bank of Kalman estimators are then derived using the criteria described in Section 2.3. The inputs to these Kalman estimators are listed in Table 1, and the outputs of these estimators are all floor accelerations. All types of faults are manually added to the 5th floor acceleration response at 16 seconds, and each fault is separately examined.

Fig. 5(a) demonstrates the comparison between the measured and estimated accelerations at the 5th floor. The estimated acceleration is derived from the Kalman estimator 5, which has the 1st-4th floor acceleration as inputs. As seen in this figure, the small errors indicate the performance of the Kalman estimator generated from the proposed procedure. Therefore, the bank of Kalman estimators can well estimate the one-step ahead acceleration responses if all sensors work normally.

Table 1 Configuration of a bank of Kalman estimators

Kalman estimator	Acceleration Inputs
Kalman estimator 1	Floors 2, 3, 4, 5
Kalman estimator 2	Floors 1, 3, 4, 5
Kalman estimator 3	Floors 1, 2, 4, 5
Kalman estimator 4	Floors 1, 2, 3, 5
Kalman estimator 5	Floors 1, 2, 3, 4

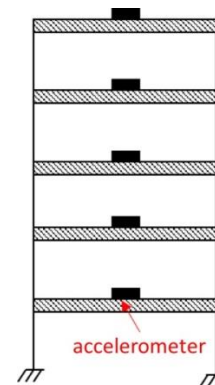


Fig. 3 Illustration of the building used in the numerical study

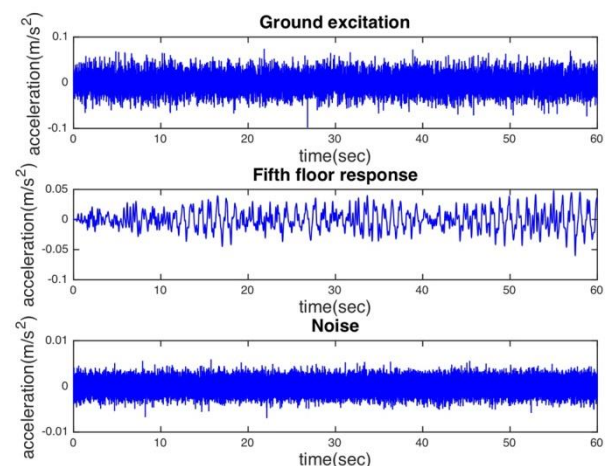
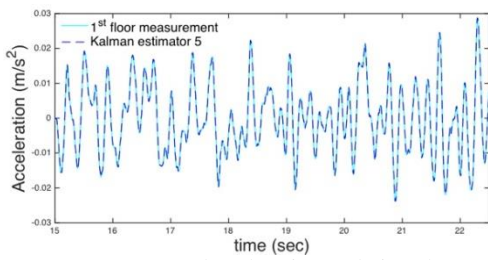
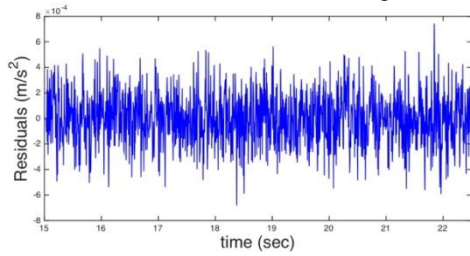


Fig. 4 Simulation results from top to bottom: ground excitation, acceleration response at the 5th floor, and sensor noise of the 5th floor accelerometer



(a) Measured and estimated signal



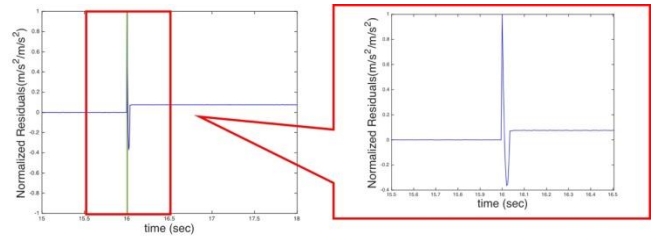
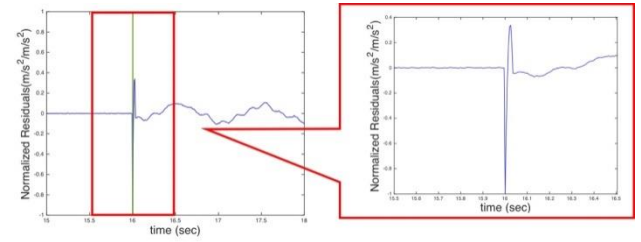
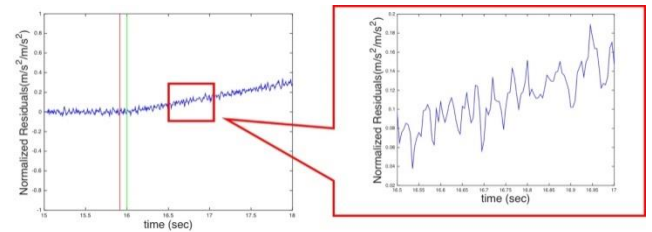
(b) Residuals between the measured and estimated signal

Fig. 5 Comparison of the 5th-floor acceleration to the estimated response from the Kalman estimator 5

In the evaluation of sensor fault detection, Figs. 6-8 show the performance of the proposed method. Note that the residual responses shown in these figures are normalized to the maximum 5th-floor acceleration that allow increased resolutions in the plots. Fig. 6 exhibits the residual time history when the additive fault occurs in the 5th-floor accelerometer. The artificially constant offset Δ_5 (see Eq. (11)) is set to be 80% of the maximum acceleration response in the 5th-floor accelerometer. As seen in this figure, the pulse is almost aligned at 16 seconds, indicating the fault occurrence. The later constant offset in the residual time history is identical to Δ_5 . In this example, the proposed method is verified to be capable of detecting the faulty sensor in terms of type and time of occurrence.

Fig. 7 demonstrates the sensor fault detection to the multiplicative fault in the 5th-floor accelerometer. The α_5 (see Eq. (12)) is set to be 1.5 that amplified the original measurements starting at 16 seconds. The pulse-like response occurs in the residual time history almost at 16 seconds, and the later residual response oscillates around zero, indicating the multiplicative fault. Therefore, the proposed method can identify the sensor with the multiplicative fault in a sensor network.

Fig. 8 displays the proposed fault detection method applied to the slowly drifting fault in the 5th-floor accelerometer. The β_5 (see Eq. (13)) is set to be 2.5×10^{-3} . As seen in the result, a constant slope is found in the residual response, indicating the slowly drift fault. The time of fault occurrence is approximated by this slope as the red line in this figure. The approximated occurrence time is slightly off to 16 seconds. For this type of faults, the proposed method can recognize the faulty sensor and fault type, while the time of fault occurrence can be only estimated.

Fig. 6 5th-floor residual time history with the additive faultFig. 7 5th-floor residual time history with the multiplicative faultFig. 8 5th-floor residual time history with the slowly drifting fault

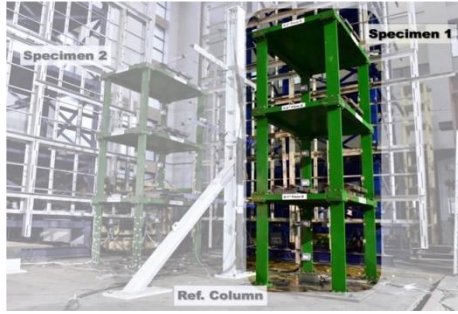
4. Experimental validation of sensor fault detection

An experimental test of a three-story steel-frame model building (see Fig. 9(a)) is carried out using shaking table testing to collect the structural responses. This model building is 3.5 m high and 2.94 ton in total. All columns are made in A36 steel with a strength of 250 MPa. Each column has the same size with a dimension of 0.15 m \times 0.025 m \times 1.06 m. In this shaking table testing, the ground excitation is applied to the weak direction of the building. The natural frequencies of this building are 2.597 Hz, 7.465 Hz, 10.02 Hz, 11.17 Hz, and 24.07 Hz. To examine the proposed method, only the acceleration responses along the weak axis are used. More details about the building geometry and instrumentation plan are available in Loh *et al.* (2016). In this study, the objective is to apply the proposed sensor fault detection method to the measured floor accelerations with artificially added faults.

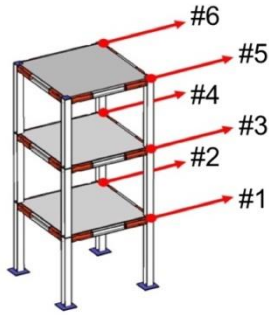
Each floor is equipped with two uniaxial accelerometers at both sides as shown in Fig. 9(b). The accelerometers used in this experiment are Setra model 141B. The measurements are sampled at 200 Hz. Both earthquake and band-limited white noise (BLWN) excitations are considered as the ground input to this building. The band-limited white noise excitation is 180 seconds long.

Table 2 Configuration of a bank of Kalman estimators

Kalman estimator	Acceleration Inputs
Kalman estimator 1	Sensors 2, 3, 4, 5, 6
Kalman estimator 2	Sensors 1, 3, 4, 5, 6
Kalman estimator 3	Sensors 1, 2, 4, 5, 6
Kalman estimator 4	Sensors 1, 2, 3, 5, 6
Kalman estimator 5	Sensors 1, 2, 3, 4, 6
Kalman estimator 6	Sensors 1, 2, 3, 4, 5



(a) Experimental building



(b) Model building and accelerometer instrumentation

Fig. 9 Illustration of the three-story experimental building and model building

Because the input excitation in the first 20 seconds is insignificant, only portion of measurements in 20-180 seconds are employed to evaluate the proposed method. All acceleration measurements generated from the BLWN are used to develop an AR model that subsequently renders as a bank of Kalman estimators. Note that all analyses offset the time histories to be 0-160 seconds. The artificial faults are separately added to the sensor measurements in order to assess the performance of the proposed method.

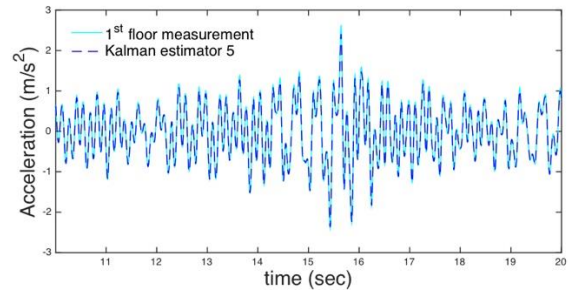
The bank of Kalman estimators are developed to be similar with the case in the numerical example. All Kalman estimators used are listed in Table 2. Each estimator has 5 inputs and 6 outputs to identify the fault of the missing one in the inputs. Fig. 10 compares the estimated acceleration at the east 1st floor (i.e., the #1 sensor in Fig. 9) to the measured one, and the Kalman estimator consists of the #1-4 and #6 sensor measurements as inputs and all floor accelerations as outputs. Because a slight DC offset exists in some sensor measurements, the minor errors between the measured and estimated floor accelerations occur at the

positive side. The proposed method is validated to derive a bank of Kalman estimators that effectively estimate sensor measurements.

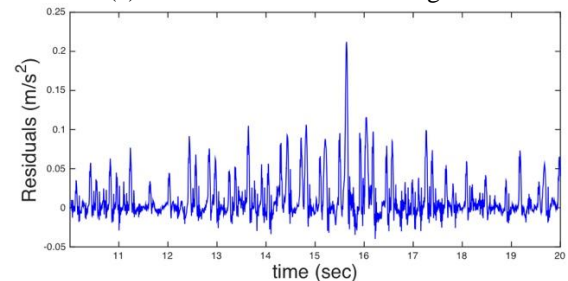
Figs. 11-13 exhibit the performance of the proposed method applied to the experimental data. In these figures, the red vertical lines denote the identified time of fault occurrence, while the green vertical lines represent the true occurrence time of the fault in the #5 sensor. As shown in Fig. 11, the proposed method is capable of detecting the additive fault in the #5 sensor. The artificially additive offset Δ_5 is set to be 500% of the maximum acceleration response in the #5 sensor. Moreover, a good agreement between the red and green lines indicates the capability of identifying the fault occurrence time.

For the multiplicative fault, the α_5 is specified to be 2 and the detection results is shown in Fig. 12. The pulse-like response occurs in the residual time history almost at 16 seconds, and the later residual response oscillates around zero. This pattern indicates the multiplicative fault in the sensor.

Fig. 13 presents the results of the proposed fault detection method in the case of the slowly drifting fault in the #5 sensor measurement. The β_5 is set to be 2.5. As seen in the result, a constant slope is found in the residual response, indicating the slowly drift fault. This slope is identical to β_5 . The approximated occurrence time is slightly off to 16 seconds. For this type of faults, the proposed method can recognize the faulty sensor and fault type, while the time of fault occurrence can be only estimated.



(a) Measured and estimated signal



(b) Residuals between the measured and estimated signal

Fig. 10 Comparison of the 1th-floor acceleration to the estimated response from a Kalman estimator 5

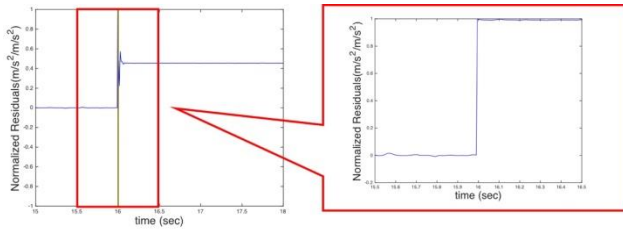


Fig. 11 5th-sensor residual time history with the additive fault

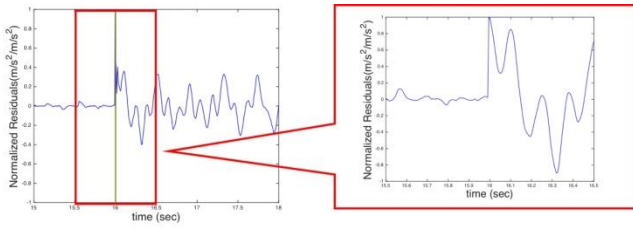


Fig. 12 5th-sensor residual time history with the multiplicative fault

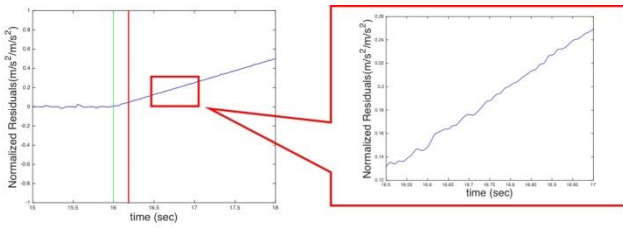


Fig. 13 5th-sensor residual time history with the slowly drifting fault

All faults are detected by the calculated residuals between the estimated and measured responses. The occurrences of faults are determined with a decent accuracy. Moreover, the proposed method also diagnoses fault types by observing the trend of residual responses after a fault occurrence.

Sensors may have re-occurring faults that the proposed method is also capable of detecting. Fig. 14 shows the sensor fault detection method for identifying multiple sensor faults. For example, the proposed method detects the additive sensor fault at the #5 sensor. The biased sensor signal at this sensor is corrected after the fault is successfully detected (i.e., at 21 seconds). The fault correction method can be carried out by a curve-fitting algorithm. Thus, the original estimator can be still used with the corrected signal as the #5 sensor measurement. Consequently, the second fault at the #6 sensor can be detected.

Fig. 15 demonstrates the proposed method to detect an additive fault which is added at 16 second on the fifth sensor and a slowly drifting fault which is added at 32 second on the sixth sensor. The Δ_5 is set to be 500% of the maximum acceleration response in the #5 sensor measurement, and the β_6 is set to be 2. The result indicates that the proposed fault detection method is capable of detecting re-occurring faults.

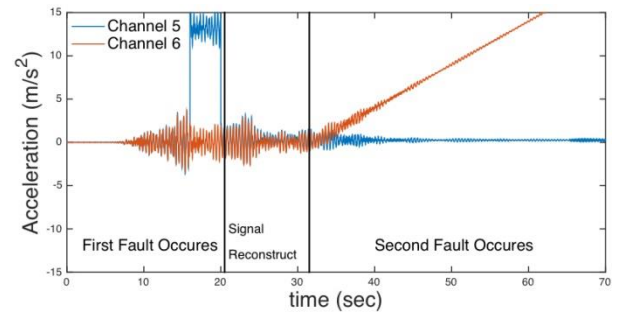
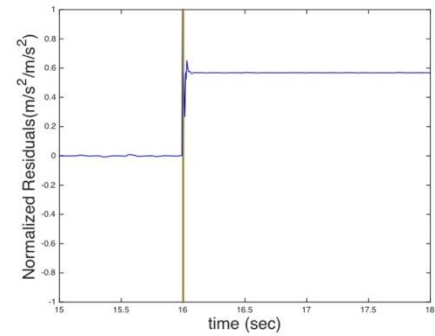
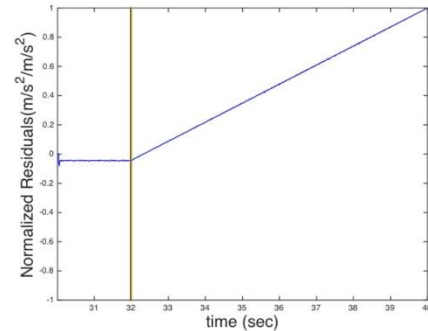


Fig. 14 Time histories of sensors with re-occurring faults



(a) 5th-sensor residual time history with the additive fault



(b) 6th-sensor residual time history with the slowly drifting fault

Fig. 15 Residual time history with re-occurring faults

5. Conclusions

This study proposed a sensor fault detection method using a bank of Kalman estimators. Three types of sensor faults were considered including the additive, multiplicative, and slowly drifting faults. The bank of Kalman estimators were converted from the autoregressive modelling to the structure using the sensor measurements. The fault detection was then realized by recognizing specific patterns in residuals, which were calculated by differentiating the measured and estimated signals. The additive fault resulted in residuals with an offset. The multiplicative fault introduced oscillating residuals around zero. The slowly drifting fault deviated residuals from zero by a linear curve. As seen in the results, the proposed method was capable of determining the fault types among these three faults. Meanwhile, this method can accurately the time of

occurrence for the additive and multiplicative fault. For the slowly drifting fault, the time of fault occurrence can be still estimated with a decent accuracy. Moreover, the sensor fault detection method was capable of detecting re-occurring faults in sensors as illustrated in the experimental example. Therefore, faulty sensors in a sensor network can be identified using the proposed sensor fault detection method, while the fault occurrences and types are concurrently determined.

Acknowledgments

This research is supported by the Ministry of Science and Technology in Taiwan under Grant No. MOST 104-2218-E-036 and MOST 105-3011-F-009-003. The authors are grateful for the experimental data shared by Professor Chin-Hsiung Loh.

References

- Abdelghani, M. and Friswell, M. (2007), "Sensor validation for structural systems with multiplicative sensor faults", *Mech. Syst. Signal Pr.*, **21**, 270-279.
- Akaike, H. (1974), "A new look at the statistical model identification", *IEEE T. Automat. Contr.*, **19**(6), 716-723.
- Akaike, H. (1977), "An objective use of Bayesian models", *Annal. Inst. Stat. Math.*, **29**, 9-20.
- Beck, J.L., Vanik, M.W., Polidori, D.C. and May, B.S. (1998), "Structural health monitoring using ambient vibrations", *Proceedings of the Structural Engineers World Congress*, Paper T118-3, San Francisco, July.
- Brownjohn, J.M.W. (2006), "Structural health monitoring of civil infrastructure", *Philos. T. R. Soc. A*, **365**, 589-622.
- Busca, G., Cigada, A. and Datteo, A. (2015), "Autoregressive model applied to the meazza stadium for damage detection", *Structural Health Monitoring and Damage Detection*, 7, conference proceedings.
- Farrar, C.R. and James, G.H., III (1997), "System identification from ambient vibration measurements on a bridge", *J. Sound Vib.*, **205**(1), 1-18.
- Feng, M.Q. (2009), "Application of structural health monitoring in civil infrastructure", *Smart Struct. Syst.*, **5**(4), 469-482.
- Hanlon, P.D. and Maybeck, S.M. (2000), "Multiple-model adaptive estimation using a residual correlation Kalman filter bank", *IEEE T. Aero. Elec. Sys.*, **36**(2), 393-406.
- Heredia, G. and Ollero, A. (2011), "Detection of sensor faults in small helicopter UVAs using observer/Kalman filter identification", *Mathematical Problems in Engineering*, 2011, ID: 174618.
- Heredia, G., Ollero, A., Bejar, M. and Mahtani, R. (2008), "Sensor and actuator fault detection in small autonomous helicopters", *Mechatronics*, **18**, 90-99.
- Kim, K., Choi, J., Koo, G. and Sohn, H. (2016), "Dynamic displacement estimation by fusing biased high-sampling rate acceleration and low-sampling rate displacement measurements using two-stage Kalman estimator", *Smart Struct. Syst.*, **17**(4), 647-667.
- Kobayashi, T. and Simon, D.L. (2005), "Evaluation of an enhanced bank of Kalman filters for in-flight aircraft engine sensor fault diagnostics", *J. Eng. Gas Turb. Power*, **127**, 497-504.
- Lei, Y., Luo, S. and Su, Y. (2016), "Data fusion based improved Kalman filter with unknown inputs and without collocated acceleration measurement", *Smart Struct. Syst.*, **18**(3), 375-387.
- Lei, Y., Chen, F. and Zhou, H. (2015), "A two-stage and two-step algorithm for the identification of structural damage and unknown excitations: numerical and experimental studies", *Smart Struct. Syst.*, **15**(1), 57-80.
- Liao, Y., Kiremidjian, A.S., Rajagopal, R. and Loh, C.H. (2016), "Angular velocity-based structural damage detection", *Sensors and Smart Structures Technologies for Civil, Mechanical, and Aerospace Systems 2016*, 9803.
- Lim, J.K. and Park, C.G. (2014), "Satellite fault detection and isolation scheme with modified adaptive fading EKF", *J. Elec. Eng. Technol.*, **9**(4), 1401-1410.
- Loh, C.H., Chan, C.K., Chen, S.F. and Huang, S.K. (2016), "Vibration-based damage assessment of steel structure using global and local response measurements", *Earthq. Eng. Struct. D.*, **45**(5), 699-718.
- Lynch, J.P., Sundararajan, A., Law, K.H., Kiremidjian, A.S. and Carryer, E. (2004), "Embedding damage detection algorithms in a wireless sensing unit for operational power efficiency", *Smart Mater. Struct.*, **13**, 800-810.
- Merrill, W.C., DeLaat, J.C. and Bruton, W.M. (1998), "Advanced detection isolation, and accommodation of sensor failures – Real-time evaluation", *J. Guid. Control Dynam.*, **11**(6), 517-526.
- Nardi, D., Lampani, L., Pasquali, M. and Gaudenzi, P. (2016), "Detection of low-velocity impact-induced delaminations in composite laminates using Auto-Regressive models", *Compos. Struct.*, **151**, 108-113.
- Palanisamy, R.P., Cho, S., Kim, H. and Sim, S.H. (2015), "Experimental validation of Kalman filter-based strain estimation in structures subjected to non-zero mean input", *Smart Struct. Syst.*, **15**(2), 489-503.
- Park, K., Kim, S. and Torbol, M. (2016), "Operational modal analysis of reinforced concrete bridges using autoregressive model", *Smart Struct. Syst.*, **17**(6), 1017-1030.
- Park, S., Yun, C.B., Ron, Y. and Lee, J.J. (2005), "Health monitoring of steel structures using impedance of thickness modes at PZT patches", *Smart Struct. Syst.*, **1**(4), 339-353.
- Pbrianti D., Mustafa, M., Abdullah, N.R.H. and Bayuaji, L. (2016), "Bank of Kalman filters for fault detection in quadrotor MAV", *Asian Research Publishing Network*, **11**(10).
- Peeters, B. and Roeck, G.D. (2001), "One-year monitoring of the Z24-Bridge: environmental effects versus damage events", *Earthq. Eng. Struct. D.*, **30**(2), 149-171.
- Qin, S.J. and Li, W. (1999), "Detection, identification, and reconstruction faulty sensors with maximized sensitivity", *AIChE J.*, **45**(9).
- Rice, J.A. and Spencer, B.F., Jr. (2009), "Flexible smart sensor framework for autonomous full-scale structural health monitoring", NSEL Report No. NSEL-018, University of Illinois at Urbana-Champaign, Champaign, IL, August.
- Saravanakumar, R., Monimozhi, M., Kothari, D.P. and Tejenosh, M. (2014), "Simulation of sensor fault diagnosis for wind turbine generators DFIG and PMSM using Kalman filter", *Energy Procedia*, **54**, 494-505.
- Sohn, H., Czarnecki, J.A. and Farrar C.R. (2000), "Structural health monitoring using statistical process control", *J. Struct. Eng. - ASCE*, **126**(11), 1356-1363.
- Wang, H., Li, L., Song, G., Dabney, J.B. and Harman, T.L. (2015), "A new approach to deal with sensor errors in structural controls with MR damper", *Smart Struct. Syst.*, **16**(2), 329-345.
- Xia, Y.X. and Ni, Y.Q. (2016), "Extrapolation of extreme traffic load effects on bridges based on long-term SHM data", *Smart Struct. Syst.*, **17**(6), 995-1015.
- Xu, Y.L., Huang, Q., Xia, Y. and Liu, H.J. (2015), "Integration of health monitoring and vibration control for smart building structures with time-varying structural parameters and unknown excitations", *Smart Struct. Syst.*, **15**(3), 807-830.

Yao, R. and Pakzad, S.N. (2012), "Autoregressive statistical pattern recognition algorithms for damage detection in civil structures", *Mech. Syst. Signal Pr.*, **31**, 355-368.

BS